Mechanisms of Microtubule Guiding on Microfabricated Kinesin-Coated Surfaces: Chemical and Topographic Surface Patterns

John Clemmens,[†] Henry Hess,[†] Ryan Lipscomb,[‡] Yael Hanein,[‡] Karl F. Böhringer,[‡] Carolyn M. Matzke,[§] George D. Bachand,[||] Bruce C. Bunker,[||] and Viola Vogel*,[†]

Department of Bioengineering and Center for Nanotechnology, Box 351721, University of Washington, Seattle, Washington 98195, Department of Electrical Engineering, Box 352500, University of Washington, Seattle, Washington 98195, Microdevice Technologies, Sandia National Laboratories, P.O. Box 5800, MS 0603, Albuquerque, New Mexico 87185, and Biomolecular Materials and Interfaces, Sandia National Laboratories, P.O. Box 5800, MS 1413, Albuquerque, New Mexico 87185

Received August 18, 2003. In Final Form: October 6, 2003

Cells regulate active transport of intracellular cargo using motor proteins. Recent nanobiotechnology efforts aim to adapt motor proteins to power the movement and assembly of synthetic materials. A motor-protein-based nanoscale transport system (molecular shuttle) requires that the motion of the shuttles be guided along tracks. This study investigates the principles by which microtubules, serving as shuttle units, are guided along micrometer-scale kinesin-coated chemical and topographical tracks, where the efficiency of guidance is determined by events at the track boundary. Thus, we measure the probability of guiding as microtubules reach the track boundary of (1) a chemical edge between kinesin-coated and kinesin-free surfaces, (2) a topography-only wall coated completely with kinesin, and (3) a kinesin-free wall next to a kinesin-coated bottom surface (topography and chemistry combined). We present a guiding mechanism for each surface type that takes into account the physical properties of microtubule filaments and the surface properties (geometry, chemistry), and elucidate the contributions of surface topography and chemistry. Our experimental and theoretical results show that track edges that combine both topography and chemistry guide microtubules most frequently (approximately 90% of all events). By applying the principles of microtubule guidance by microfabricated surfaces, one may design and build motor-protein-powered devices optimized for transport.

Introduction

Over millions of years, cells have evolved molecular machinery to carry out complex transport processes necessary for cell survival. Active transport in cells is driven by the conversion of chemical energy stored in ATP into mechanical work by motor proteins (e.g., kinesin), which move along protein filaments (e.g., microtubules). Current efforts to synthesize molecular motors[1] have not yet delivered an engine comparable in efficiency and size to biomolecular motors, which has fueled the interest in hybrid nanodevices that integrate biomolecular motors.[2,3] An example of such a hybrid nanodevice is the concept of a "molecular shuttle", a nanoscale transport system driven by the motor protein kinesin.[3−5]

Recently, several strategies to build microscopic tracks for molecular shuttles and related hybrid systems have been proposed. Derived from the "gliding motility assay",[6] filaments glide on motor-protein-coated surfaces (Figure 1), where tracks have been created by various patterning methods.[4,5,7−12] Alternatively, motor proteins can carry cargo while walking on an ordered array of surface-immobilized filaments,[13−15] similar to the "bead motility assay".[16] Spatial and temporal control of a transport system in general requires that motion be confined along tracks (Figure 1); thus the gliding motility assay modified with microfabricated surfaces[5,8−11,17,18] holds an advantage over the bead orientation in the ability to create complex

* Corresponding author. Voice: 206-543-1776. Fax: 206-685-4434. E-mail: vvogel@u.washington.edu.

[†] Department of Bioengineering and Center for Nanotechnology, University of Washington.

[‡] Department of Electrical Engineering, University of Washington.

[§] Microdevice Technologies, Sandia National Laboratories.

[||] Biomolecular Materials and Interfaces, Sandia National Laboratories.

(1) Balzani, V.; Credi, A.; Raymo, F. M.; Stoddart, J. F. *Angew. Chem., Int. Ed.* **2000**, *39*, 3349−3391.

(2) Montemagno, C.; Bachand, G. *Nanotechnology* **1999**, *10*, 225−231.

(3) Hess, H.; Vogel, V. *Rev. Mol. Biotechnol.* **2001**, *82*, 67−85.

(4) Dennis, J. R.; Howard, J.; Vogel, V. *Nanotechnology* **1999**, *10*, 232−236.

(5) Hess, H.; Clemmens, J.; Qin, D.; Howard, J.; Vogel, V. *Nano Lett.* **2001**, *1*, 235−239.

(6) Yanagida, T.; Nakase, M.; Nishiyama, K.; Oosawa, F. *Nature* **1984**, *307*, 58−60.

(7) Suzuki, H.; Oiwa, K.; Yamada, A.; Sakakibara, H.; Nakayama, H.; Mashiko, S. *Jpn. J. Appl. Phys., Part 1* **1995**, *34*, 3937−3941.

(8) Suzuki, H.; Yamada, A.; Oiwa, K.; Nakayama, H.; Mashiko, S. *Biophys. J.* **1997**, *72*, 1997−2001.

(9) Riveline, D.; Ott, A.; Julicher, F.; Winkelmann, D. A.; Cardoso, O.; Lacapere, J. J.; Magnusdottir, S.; Viovy, J. L.; Gorre-Talini, L.; Prost, J. *Eur. Biophys. J.* **1998**, *27*, 403−408.

(10) Nicolau, D. V.; Suzuki, H.; Mashiko, S.; Taguchi, T.; Yoshikawa, S. *Biophys. J.* **1999**, *77*, 1126−1134.

(11) Hiratsuka, Y.; Tada, T.; Oiwa, K.; Kanayama, T.; Uyeda, T. Q. *Biophys. J.* **2001**, *81*, 1555−1561.

(12) Hess, H.; Clemmens, J.; Matzke, C. M.; Bachand, G. D.; Bunker, B. C.; Howard, J.; Vogel, V. *Appl. Phys. A* **2002**, *75*, 309−313.

(13) Turner, D. C.; Chang, C.; Fang, K.; Brandow, S. L.; Murphy, D. B. *Biophys. J.* **1995**, *69*, 2782−2789.

(14) Bohm, K. J.; Stracke, R.; Muhlig, P.; Unger, E. *Nanotechnology* **2001**, *12*, 238−244.

(15) Limberis, L.; Stewart, R. J. *Nano Lett.* **2001**, *1*, 277−280.

(16) Spudich, J. A.; Kron, S. J.; Sheetz, M. P. *Nature* **1985**, *315*, 584−586.

10.1021/la035519y CCC: $25.00
Published on Web 11/26/2003

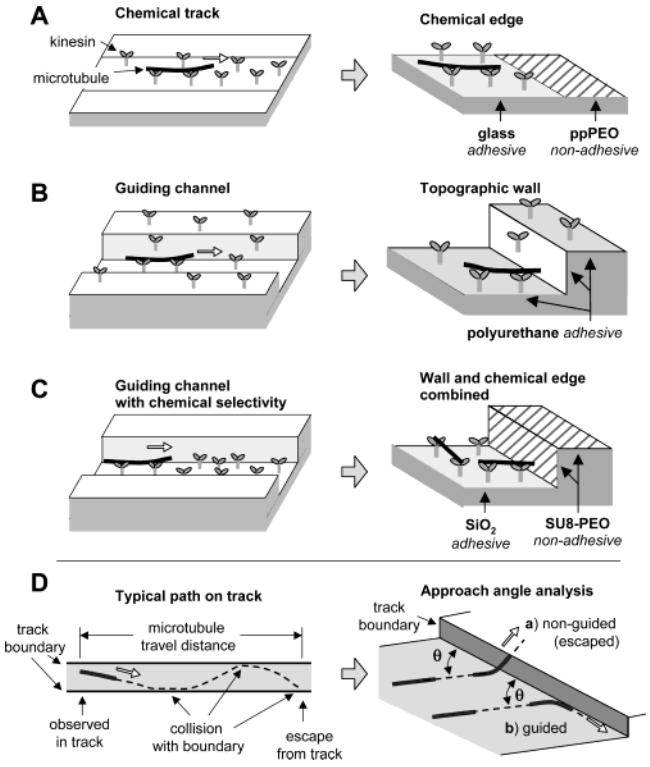

Figure 1. Strategies to surface-engineer tracks for molecular motors (left) and the corresponding test surfaces (right) used for studying guiding at track boundaries. Each surface is labeled according to its adhesiveness for kinesin. (A) Microtubules move along a chemical track of patterned kinesin surrounded by a kinesin-free surface. In all cases, the direction of microtubule gliding is determined by the microtubule polarity rather than the orientation of kinesin on the surface. Guiding is measured at a chemical edge between kinesin-adhesive (glass) and nonadhesive (ppPEO) regions. (B) Guiding channels use walls to guide the motion of microtubules along the bottom of the channel. A single wall (polyurethane) is tested for its ability to guide microtubules along the bottom surface. (C) An engineered surface that combines a guiding channel and a chemical track will use walls and patterned kinesin to move microtubules along its track. A single wall (SU8−PEO) that does not adsorb kinesin is tested for its ability to guide microtubules along the bottom surface. (D) A typical path of a microtubule as it moves along a track. The outcome of a microtubule collision with the track boundary is a key determinant of the total travel distance on the track. Microtubule collisions with the boundaries are analyzed by measuring the angle of approach θ and the outcome of the collision: (a) not guided or (b) guided.

user-defined tracks and to transport microtubules long distances (hundreds of micrometers). The various microfabricated surfaces tested to date have all been described qualitatively to guide the motion of filaments.[4,5,7−12,17,18] Represented in Figure 1, these surfaces are created by (a) a chemical pattern to selectively adsorb the motor proteins,[10] (b) a topographical pattern to create guiding channels,[5,9,17,19] or (c) a combination of selective adsorption and guiding channels.[11,18]

Our recent efforts[19] have focused on characterizing track parameters that affect guidance (Figure 1D), for example, the channel width for its effect on the distance of microtubule gliding along a kinesin-coated open channel (Figure 1B). Our findings indicate that track parameters, such as track width, determine the frequency with which microtubules approach the track edge, while the properties of the edge influence the retention of the microtubule on the track. Thus, microtubules must be frequently guided at the track edge to travel long distances on a track. To separate effects of track width from edge guiding, we analyze here quantitatively what happens when a microtubule reaches the track edge of a chemical pattern, an open channel, or a chemical pattern at the bottom of an open channel. With this detailed measure, we establish a consistent comparison of each type of surface modification for the design of microscopic tracks. We also gain insight into the mechanism of guiding for each type of surface and uncover how tracks may be optimized for increased transport efficiency. Thus, we establish a quantitative understanding of why some tracks work better than others. Taking a quantitative approach is significant for establishing design guidelines to engineer tracks for the next generation of nanodevices.

Methods

Kinesin and Microtubule Preparation. Kinesin preparation is described in detail elsewhere.[20] Briefly, a kinesin construct consisting of the wild-type, full-length *Drosophila melanogaster* kinesin heavy chain and a C-terminal His tag was expressed in *Escherichia coli* and purified using a Ni^{2+}-NTA column. The eluent contained functional motors with a concentration of ~100 nM and was used as the stock solution. A green fluorescent protein (GFP)−kinesin fusion protein (a gift from Jonathon Howard) was also used in surfaces which contained chemical-only patterns in order to visualize selective adsorption of kinesin.

Fluorescent-labeled tubulin (Cytoskeleton, Denver, CO) was polymerized into microtubules in BRB80 buffer (80 mM Pipes, 2 mM $MgCl_2$, 1 mM EGTA, pH 6.85 with KOH) with 4 mM $MgCl_2$, 1 mM GTP, and 5% DMSO for 30 min at 37 °C. Microtubules with lengths between 2 and 20 μm were 100-fold diluted and stabilized in BRB80 and 10 μM Taxol (Sigma, St. Louis, MO).

Preparation of ppPEO Chemical Patterns. Poly(ethylene oxide) (PEO) monomers (tetraethylene glycol dimethyl ether) are polymerized onto a surface by glow charge plasma deposition.[21] The resulting plasma-polymerized films (ppPEO) have been studied for their ability to resist protein adsorption.[21,22] The deposition process has recently been adapted to create patterned films of ppPEO on glass substrates.[23,24] Briefly, photoresist AZ1512 (Clariant, Somerville, NJ) is exposed through a chrome mask and developed. A thin film of ppPEO is deposited and is partially removed via photoresist lift-off to expose bare glass regions that were protected by the photoresist. The resultant surface adsorbs proteins such as kinesin in bare glass regions while remaining free of protein where the ppPEO film remains. The test surface was a straight edge of ppPEO film on glass that was separated by at least 150 μm from other patterns to reduce the effect of nonboundary patterns on the microtubule path.

The ppPEO film at the boundary is ~20 nm thick[24] and was verified on the test surfaces by atomic force microscopy. Although kinesin holds the microtubule above the surface at a height estimated to be as low as ~10 nm[25] or measured by electron microscopy as ~20 nm,[26] results from Stracke and co-workers[27]

(17) Bunk, R.; Klinth, J.; Montelius, L.; Nicholls, I.; Omling, P.; Tagerud, S.; Mansson, A. *Biochem. Biophys. Res. Commun.* **2003**, *301*, 783−788.
(18) Moorjani, S. G.; Jia, L.; Jackson, T. N.; Hancock, W. O. *Nano Lett.* **2003**, *3*, 633−637.
(19) Clemmens, J.; Hess, H.; Howard, J.; Vogel, V. *Langmuir* **2003**, *19*, 1738−1744.
(20) Coy, D. L.; Wagenbach, M.; Howard, J. *J. Biol. Chem.* **1999**, *274*, 3667−3671.
(21) Lopez, G. P.; Ratner, B. D.; Tidwell, C. D.; Haycox, C. L.; Rapoza, R. J.; Horbett, T. A. *J. Biomed. Mater. Res.* **1992**, *26*, 415−439.
(22) Shen, M. C.; Pan, Y. V.; Wagner, M. S.; Hauch, K. D.; Castner, D. G.; Ratner, B. D.; Horbett, T. A. *J. Biomater. Sci., Polym. Ed.* **2001**, *12*, 961−978.
(23) Goessl, A.; Garrison, M. D.; Lhoest, J. B.; Hoffman, A. S. *J. Biomater. Sci., Polym. Ed.* **2001**, *12*, 721−738.
(24) Hanein, Y.; Pan, Y. V.; Ratner, B. D.; Denton, D. D.; Bohringer, K. F. *Sens. Actuators, B* **2001**, *81*, 49−54.
(25) Hunt, A. J.; Howard, J. *Proc. Natl. Acad. Sci. U.S.A.* **1993**, *90*, 11653−11657.
(26) Miller, R.; Lasek, R. *J. Cell Biol.* **1985**, *101*, 2181−2193.

argue that it is unlikely that the wall height of ~20 nm contributes to guiding given the ability of microtubules to climb walls <100 nm high. Thus, we do not expect there to be a significant guiding effect due to the thickness of the ppPEO film.

Preparation of Polyurethane Topography Patterns. Replica molding[28] was used to imprint topography features into polyurethane with high fidelity. Briefly, a silicon wafer was coated with photoresist SU8-2 (MicroChem Corp., Newton, MA) and then exposed and developed to form a patterned photoresist on silicon. This surface was imprinted into poly(dimethylsiloxane) (PDMS; Dow Chemical, Midland, MI) and cured. Finally PDMS was imprinted a second time into polyurethane (NOA 73; Norland Products, Cranbury, NJ) with a cover glass backing (Corning) for support and was cured with ultraviolet light. The resulting surface had straight single walls (~1 μm high) of the same pattern as the silicon surface but had uniform polyurethane chemistry throughout. The polyurethane chemistry uniformly adsorbs kinesin such that microtubules can glide on all surfaces (the wall, the surface below the wall, and the surface above the wall). Each topography-only wall was separated by at least 150 μm from other features.

Preparation of SU8−PEO Combined Patterns. SU8-2 photoresist was spun (~4000 rpm) on a thermally grown silicon oxide surface, resulting in a 1−1.5 μm thick film. The resist was exposed through a chrome mask (Photosciences, Torrance, CA) and developed in acetone. A brief hydrofluoric etch (~5 s) into the SiO_2 surface was used to remove residual resist. A PEO triblock copolymer called Pluronic F108 (BASF, Mount Olive, NJ) [$PEO_{129}-PPO_{56}-PEO_{129}$; where PEO = poly(ethylene oxide), PPO = poly(propylene oxide)] was used to coat hydrophobic surfaces to make them nonadhesive to proteins.[29] A patterned SU8-2 surface (hydrophobic) was coated selectively by a solution of F108 (2 mg/mL in water) to make a surface kinesin-adhesive in SiO_2 regions and nonadhesive in PEO-coated SU8-2 regions (SU8−PEO). Test surfaces were rinsed twice with water and once with a buffer of BRB80 before coating with motor proteins as described below.

Motility Assay. To allow fluid exchange and visualization, test surfaces were assembled into flow cells by sandwiching no. 00 coverslips (~80 μm thick) between the test surfaces and glass slides or glass coverslips (Fisher Scientific, Pittsburgh, PA) sealed with vacuum grease. The buffer for all experiments was BRB80 (80 mM Pipes, 2 mM $MgCl_2$, 1 mM EGTA, pH 6.85 with KOH). The flow cells were sequentially filled with a casein solution (0.5 mg/mL casein in BRB80), a solution containing 0.2 mg/mL casein, 1 mM ATP, and kinesin (10 μg/mL for polyurethane surfaces; 2 μg/mL for all other surfaces) in BRB80, and finally a motility solution [~3.2 μg/mL of tetramethylrhodamine-labeled microtubules (1−10 μm in length) containing 1 mM ATP and stabilized by 10 μM Taxol with oxygen-scavenging additives (20 mM D-glucose, 20 μg/mL glucose oxidase, 8 μg/mL catalase, and 0.2% 2-mercaptoethanol)]. A stochastic detachment rate of microtubules from surface boundaries that is dependent on kinesin density could potentially skew guiding results. Therefore, experiments were conducted at a high motor density such that microtubules were not observed to detach spontaneously from control surfaces. The assays were performed at ambient temperature (19 °C). Microtubules were visualized on the patterned surface by a Leica DM-IRBE fluorescent microscope (Leica AG, Wetzlar, Germany) using rhodamine filters.

Boundaries were determined from transmission microscopy images (topography-only polyurethane wall) or fluorescence microscopy images using the fluorescein filters (ppPEO chemical edge; SU8−PEO wall and chemical edge combined). For each region, sequential images of microtubules gliding along the surface were captured using an Orca2 cooled-CCD camera (Hamamatsu Photonics, Hamamatsu, Japan) with an imaging area of 64 × 80 μm^2. Microtubule positions were tracked with Metamorph image analysis software (Universal Imaging, Downingtown, PA). Approximately 200 microtubules were analyzed for each surface type; these were pooled from at least four boundaries on two preparations of each surface type (i.e., topography-only polyurethane wall, ppPEO chemical edge, and SU8−PEO wall and chemical edge combined).

Approach Angle Analysis. Image analysis consisted of measuring coordinates for the topographical, chemical, or combined boundary and the endpoints of the microtubules one image before crossing or colliding with the boundary. The microtubule coordinates were used to calculate an approach angle, θ, relative to the boundary as illustrated in Figure 4 (5 s) and Figure 5 (10 s). A guiding event occurred if the microtubule aligned itself with the boundary and remained traveling on the bottom surface for at least 10 μm. A microtubule was not considered guided if (1) it detached from the surface after hitting the wall, (2) climbed up the wall, or (3) detached from the surface after crossing the chemical boundary. Microtubules could collide multiple times with the same boundary and were only counted for multiple collisions if they traveled at least 0.5 μm away from the boundary or traveled more than 20 μm along the boundary. The approach angles were sorted into a histogram at each 10° interval. For each interval, the probability of guiding was calculated as the ratio of guided events to the total number of microtubules hitting the boundary on the interval. Standard errors were determined for the probabilities by the formula $SE = (p(1-p)/N)^{0.5}$, where p is the probability of guiding and N is the total number of microtubules colliding on that interval.

Results

Verifying Chemistry and Topography of Test Surfaces. We demonstrate selective adsorption of kinesin to glass versus the ppPEO chemical pattern (1) by microtubule binding assays and (2) by imaging the fluorescence of GFP-kinesin. First, at the kinesin concentrations used, control glass surfaces supported motility, while ppPEO-coated glass surfaces did not bind microtubules nor show microtubule gliding (Figure 1A); this was tested both in the presence and absence of ATP in the motility assay solutions. The presence of a single functional kinesin can bind and translate microtubules,[30] suggesting that the adsorption of functional kinesin on ppPEO films is very low. Second, using a GFP−kinesin fusion protein in place of wild-type kinesin, we were able to monitor directly the amount of surface-adsorbed kinesin. At the ppPEO chemical edge, we noted that GFP fluorescence patterns matched glass regions and the regions binding and transporting microtubules (Figure 2A,B). Microtubules bound and moved only on GFP-kinesin regions, consistent with kinesin adsorbing selectively to the bare glass regions rather than the ppPEO film. These observations are consistent with others[21,22] who show low amounts of other proteins adsorbing on ppPEO films.

Patterns imprinted into polyurethane were verified to have walls approximately 1 μm high with a wall steepness of $\sigma \approx 70-80°$ (Figure 3A). Both upper and lower surfaces of polyurethane, as well as the wall face, were observed to move microtubules (Figure 2C), suggesting that the entire polyurethane surface adsorbed kinesin.

Analysis of SU8−PEO patterns showed we successfully created walls (topography) combined with selective kinesin adsorption (chemistry). Scanning electron microscopy imaging of SU8 test surfaces verified the presence of 1 μm high walls and measured their steepness to be $\sigma \approx 90°$ (Figure 3B). Control experiments showed that PEO triblock polymer adsorption to hydrophobic silane-treated glass or SiO_2 greatly reduced surface-bound kinesin, consistent with control experiments by others.[29] Hydrophobic SU8-2 surfaces not coated with PEO supported microtubule binding and movement at the kinesin con-

(27) Stracke, P.; Bohm, K. J.; Burgold, J.; Schacht, H. J.; Unger, E. *Nanotechnology* **2000**, *11*, 52−56.
(28) Xia, Y. N.; Rogers, J. A.; Paul, K. E.; Whitesides, G. M. *Chem. Rev.* **1999**, *99*, 1823−1848.
(29) Ho, C. H.; Limberis, L.; Caldwell, K. D.; Stewart, R. J. *Langmuir* **1998**, *14*, 3889−3894.
(30) Howard, J.; Hudspeth, A. J.; Vale, R. D. *Nature* **1989**, *342*, 154−158.

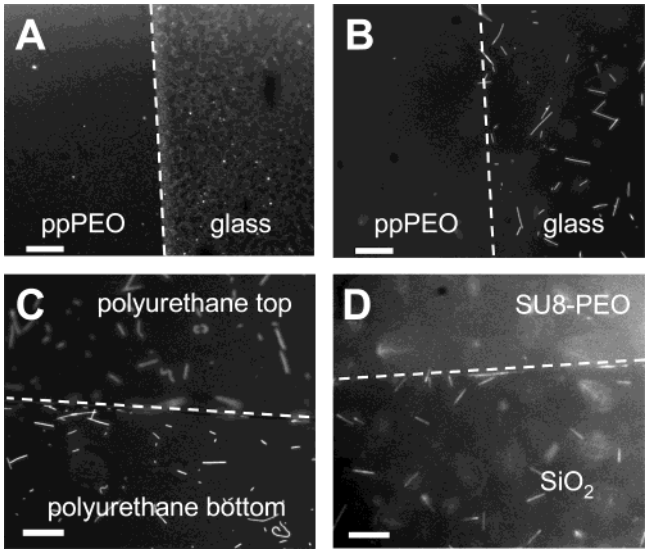

Figure 2. (A) GFP−kinesin preferentially binds to glass regions in ppPEO/glass chemical patterns as detected by fluorescence microscopy. Fluorescent speckles are presumably due to aggregated nonmotile kinesin that adsorbed to the surfaces from the kinesin solution. (B) Microtubules bind and move selectively on glass regions but do not bind or move along ppPEO regions. (C) Microtubules bind and move on all surfaces on the topography-only wall of polyurethane, suggesting that kinesin adsorbs to the entire surface. (D) SU8 treated with PEO triblock polymer also prevents microtubule binding and movement, as microtubules bind and move along SiO_2 regions. Microtubules not bound to the surface appear blurred due to the opposing orientation of the test surface and the microscope objective. The dashed line indicates the ppPEO/glass chemical edge in images A and B, the polyurethane wall in image C, and the SU8−PEO/SiO_2 wall and chemical edge in image D. Scale bar = 10 μm.

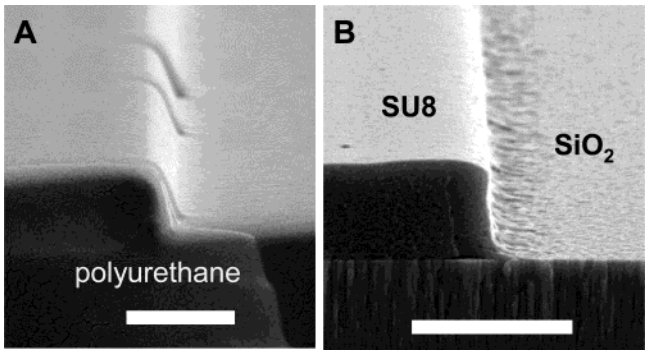

Figure 3. Scanning electron micrographs of (A) the polyurethane wall (topography only) and (B) the SU8−PEO wall on SiO_2 (combined topography and chemistry) verify the geometry of the wall at the boundary. Scale bar = 2 μm.

centration tested, thus indicating kinesin adsorption. This finding is consistent with observed properties of PEO triblock polymer to reduce adsorption of proteins on hydrophobic surfaces[29] comparable to other PEO-terminated surfaces.[31,32] In motility assays, we observed that SU8−PEO bound less than 1% of the microtubule density compared to SiO_2, and microtubule movement occurred only on the SiO_2 surface (Figure 2D), verifying a differential kinesin binding affinity due to the different surface chemistry.

Microtubule Guiding by a ppPEO Chemical Boundary on a Planar Surface. Microtubules gliding on the kinesin-coated glass region were tracked as they crossed the boundary into the kinesin-free ppPEO region (Figure 1A and Figure 4). These collisions were recorded and used to calculate the probability of microtubule guiding over a range of approach angles as shown in Figure 6A. The majority of microtubules (~88%) detached from the surface as they crossed from the glass into the ppPEO region as shown in Figure 4. Microtubules approaching the ppPEO edge from the glass region were guided by a narrow range of approach angles. For very shallow angles (<10°), microtubules were nearly always guided by slight bending, while collisions at larger angles (>30°) rarely resulted in guiding (Figure 6A). The ppPEO/glass boundary could guide microtubules by a slight bending (<20°) of the microtubule's leading tip such that the microtubule remained on the glass portion of the surfaces.

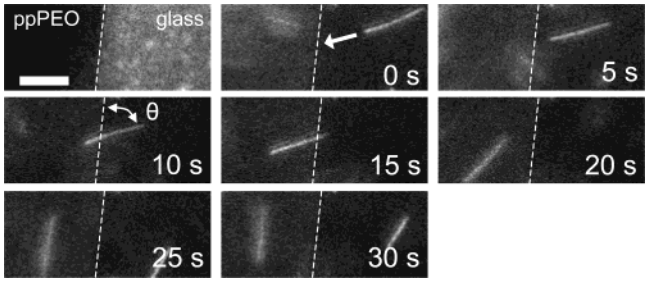

Figure 4. A microtubule detaching at a chemical (ppPEO/glass) boundary. The GFP−kinesin fluorescent pattern is imaged (upper left panel) to verify selectivity adsorption of kinesin and to define the chemical edge (dashed line). A microtubule glides on the kinesin-coated glass surface toward the kinesin-free ppPEO region (0 s). The approach angle θ is measured as the microtubule approaches the ppPEO/glass boundary (10 s). As the microtubule crosses into the ppPEO region, it partially detaches from the surface (15 s), before detaching completely (20 s) and diffusing away from the surface (25 s, 30 s). Scale bar = 10 μm.

Occasionally, we observed microtubules that were temporarily or permanently stuck to the chemical edge. Presumably this occurred through the attachment of nonmotile kinesin to the microtubule, where the trailing end bound to a nonmotile kinesin at the chemical edge. These microtubules were able to "swivel"[25] around that anchor point and sample the surface. If the sampled area is wide enough for the microtubule to bind functional kinesin near the boundary, the microtubule could continue gliding driven by these functional kinesin motors. We estimate the sweep area due to thermal fluctuations of a microtubule end-bound by a single kinesin to the surface using the swiveling model of ref 25. Assuming a drag coefficient[25] acting on the microtubule per unit length of 9.4×10^{-3} N s m^{-2}, a 5 μm long microtubule swiveling along its end for 10 s can sweep out an angle on the order of 25°. To minimize guiding artifacts from nonmotile kinesin that contribute guiding events at large approach angles, we did not include microtubules which remained stuck for 10 s or longer. To be consistent in our analysis of guiding characteristics on the chemical edge, we consider models that assume only functional motors.

Microtubule Guiding by a Polyurethane Wall with Uniform Surface Chemistry. Microtubules gliding on the bottom surface were tracked as they collided with a kinesin-coated polyurethane wall (Figure 1B). These collisions were recorded and used to calculate the probability of microtubule guiding over a range of approach angles as shown in Figure 6B. Results from this approach angle analysis agree with our previous findings[19] and show a decrease in the probability of guiding from $p \approx 50\%$ for microtubules approaching the wall at shallow angles

(31) Sofia, S. J.; Premnath, V.; Merrill, E. W. *Macromolecules* **1998**, *31*, 5059−5070.
(32) Malmsten, M.; Emoto, K.; Van Alstine, J. M. *J. Colloid Interface Sci.* **1998**, *202*, 507−517.

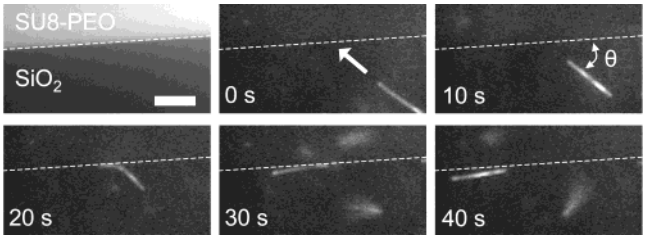

Figure 5. Microtubule guiding by a wall of SU8−PEO. SU8 auto-fluoresces under illumination and is used to determine the orientation of a wall of kinesin-free PEO-treated SU8 (light) on a kinesin-coated SiO_2 surface (dark) in the upper left panel (dashed line). A guided microtubule approaches the wall at angle θ (0 s, 10 s) and undergoes bending (20 s) until it is aligned with the wall (30 s) and proceeds along the bottom surface (40 s). Scale bar = 5 μm.

(<30°) to $p \approx 0\%$ for orthogonal approach angles. A topography-only wall could bend the microtubule's leading tip into alignment, particularly for those microtubules approaching at shallow angles. Because all surfaces (including the wall) are coated with kinesin, two paths of travel are possible for the microtubule once aligned to the base of the wall: (1) climbing up the wall (escaping) and (2) traveling along the bottom surface (guiding). Each of these paths is equally possible at shallow approach angles as shown by ~50% guiding probability per collision.

In some cases, microtubules traveled along the edge where the wall and bottom surface meet following a collision with the wall. At this edge, a microtubule may interact with kinesin on both wall and bottom surfaces, which potentially causes a preference of the microtubules for the edge over climbing the wall. If these microtubules travel long enough to be counted as guided according to our guiding criteria (>10 μm), they may increase the probability of guiding above $p = 50\%$ for the shallowest approach angles.

Generally, microtubules at large approach angles (>30°) were guided more frequently than observed for the ppPEO chemical edge. The guiding probability for the topography-only walls dropped linearly rather than exponentially as for the glass−ppPEO boundaries (Figure 6B). We propose this is due to the increased bending of microtubules by the wall compared to the chemical boundary.

Microtubule Guiding by a PEO Chemical Edge Combined with a Wall of SU8. Microtubules gliding on the kinesin-coated SiO_2 bottom surface were tracked as they collided with a kinesin-free wall of PEO-treated SU8 (Figure 1C and Figure 5). These collisions were recorded and used to calculate the probability of microtubule guiding over a range of approach angles as shown in Figure 6C. Similar to results for polyurethane walls, the SU8−PEO wall could guide microtubules by bending the leading tip of the microtubule (Figure 5). In conjunction with PEO treatment, however, guiding occurred at all approach angles, and microtubules could bend more sharply to accommodate guiding. As a result, we observed a guiding probability of $p \approx 0.9$ for all approach angles as shown in Figure 6C. This result is consistent with experiments performed by Hiratsuka et al.[11] who reported that microtubules were rarely observed to climb a 1 μm high wall with characteristics similar to our combined surfaces (made using photoresist SAL601). For SiO_2/SU8 control surfaces where PEO triblock polymer was not added and where presumably there is some kinesin adsorbed to the wall, we noted that some microtubules could escape over the wall. The lack of chemical selectivity reduced the probability of guiding for all angles in this case.

Evidently, guiding may be drastically improved by the selective adsorption of kinesin to the bottom of tracks if the microtubule is aligned with the wall. In this case, the microtubule movement up the wall will be due solely to fluctuations of the microtubule tip; however, the affinity of the microtubule for kinesin causes the tip to return to and continue moving along the bottom surface. This is in contrast to polyurethane (topography-only) walls, which have kinesin adsorbed to the wall face and support movement up the wall, thus reducing guiding probability.

Discussion

From our approach angle analysis, we found that (1) chemical patterns of kinesin only guide at shallow approach angles, (2) topography-only walls guide only half the time at shallow angles and guiding drops off linearly with increasing approach angle, and (3) combined patterns (topography and chemical) yield the most guiding events ($p \approx 0.9$) independent of the approach angle of microtubules. We aim to understand the mechanism of guiding by determining how a chemical edge and a wall contribute to guiding. Therefore, we have derived models that incorporate the material properties of microtubules and wall geometry to predict results consistent with our observations.

Estimating Microtubule Guiding Due to Thermal Fluctuations at a Chemical Boundary. In chemical patterns, a microtubule that partially crosses onto a ppPEO region is free to fluctuate, because it is bound only by kinesin on the glass surface. Without a physical boundary such as a wall to push against the free end of the microtubule, microtubule bending originates only from fluctuations by the microtubule tip due to Brownian motion. The fluctuating microtubule tip sweeps out an area on the surface and is guided if the microtubule approaches at a shallow enough angle such that its overhanging portion can bend back into the glass region where it can resume gliding (Figure 7).

The amount of bending can be determined from the stiffness of the microtubule and the amount of time the microtubule is given to fluctuate. These two parameters are measured by the flexural rigidity (EI) and the first passage time (t_k). In this case, the first passage time is the average time that a microtubule free tip takes to deflect a given distance. Small deflections will have short first passage times, while larger deflections will take long times, with the exact relationship depending on the energy required for the large deflections. The first passage time for a fluctuating particle can be written[33] as

$$t_k = \tau\sqrt{\frac{\pi}{4}}\sqrt{\frac{kT}{U_0}}\exp\left(\frac{U_0}{kT}\right) \qquad \text{for } U_0 \gg kT \qquad (1)$$

where U_0 is the elastic energy of the particle and τ is the relaxation time. The elastic energy U_0 for a microtubule which bends in the guided path (Figure 7C) is

$$U_0 = EI\frac{L}{2R^2} = \frac{2EI}{L}\tan^2\theta \qquad (2)$$

where L is the overhang length, R is the radius of curvature of the bend with $R \approx L^2/8h$,[19] h is the tip displacement, and θ is the approach angle with $\tan\theta = 4h/L$. The

(33) Howard, J. *Mechanics of motor proteins and the cytoskeleton*; Sinauer Associates: Sunderland, MA, 2001.

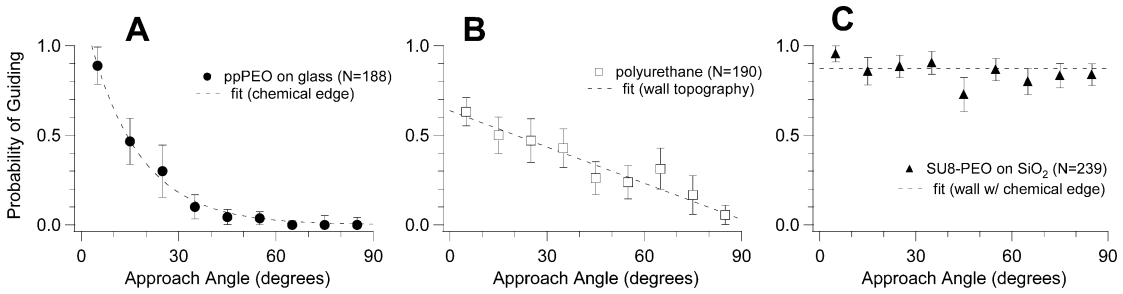

Figure 6. Probability of guiding for various microtubule approach angles at (A) a ppPEO/glass chemical boundary, (B) a polyurethane wall (topography), and (C) a combined chemical edge and topographical wall of SU8−PEO and SiO_2 (shown ± standard errors). The probability drops according to the least-squares fit equations (A) $y = 1.2\ \exp(-0.064x)$, (B) $y = 0.64 - 0.0067x$, and (C) $y = 0.87$ (N = number of total collisions; bin width = 10°).

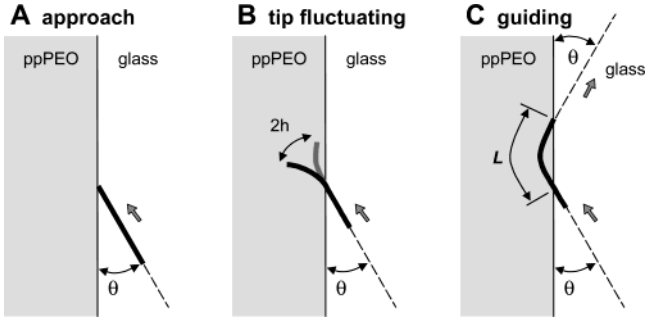

Figure 7. Schematic of guiding by microtubule bending at a chemical boundary. (A) A microtubule approaches the chemical boundary and (B) undergoes thermal fluctuations of its free tip (of amplitude h) in the ppPEO region, which does not contain kinesin. (C) For microtubules approaching at a shallow angle θ, the fluctuations provide enough bending (through a microtubule length L) for the tip to reach the glass region and continue gliding.

relaxation time τ is estimated in Gittes et al. (1993) as

$$\tau \approx \frac{\gamma}{EI}\left(\frac{L}{\pi(n+(1/2))}\right)^4 = \frac{\gamma}{EI}\left(\frac{2L}{3\pi}\right)^4 \quad (n = 1, \text{first mode only}) \quad (3)$$

where γ is the perpendicular drag coefficient, L is the overhang length of the microtubule fluctuating, and n is the bending mode. For this calculation, we consider only the first bending mode ($n = 1$) since it will contribute the most to the deflection. Furthermore, the perpendicular drag coefficient per unit length γ can be approximated by the formula for a cylinder moving near a surface,[25]

$$\gamma = \frac{4\pi\eta}{\operatorname{arccosh}\left(1 + \frac{b}{r}\right)} \quad (4)$$

where η is the viscosity ($\eta = 1.03 \times 10^{-3}$ kg m^{-1} s^{-1} for water at 19 °C), b is the height of the cylinder axis to the surface [estimated at ~11 nm[25]], and r is the hydrodynamic radius [$r \approx 15$ nm for microtubules;[25] if the ppPEO layer decreases the distance between surface and microtubule, this would lead to fewer guiding events as the drag increases and the tip fluctuations are reduced]. Rewriting eq 1 in terms of the microtubule overhang length L and approach angle θ, we have

$$t_k = \frac{\gamma}{EI}\left(\frac{2L}{3\pi}\right)^4 \sqrt{\frac{\pi}{4}}\sqrt{\frac{kT}{2EI}\frac{L}{\tan^2\theta}}\exp\left(\frac{2EI}{kT}\frac{\tan^2\theta}{L}\right) \quad (5)$$

According to eq 5, the time t_k needed for thermal fluctuations to bend a microtubule by an angle θ will increase dramatically as the approach angle θ increases. Initially, t_k will decrease when the overhang length L increases due to the decreased elastic energy barrier; however, it will increase as L continues to increase due to the increase in the relaxation time (τ).

For the average microtubule to be guided, the first passage time t_k must be within the time that a microtubule has to sample the surface. Assuming a microtubule travels at ~0.5 μm/s, it will have approximately $t_k = 10$ s to sample the surface until it overhangs by $L = 5$ μm (average microtubule length). Using $EI \approx 30 \times 10^{-24}$ N m^2,[34] we calculate $\tau = 0.5$ ms for a microtubule overhang of length $L = 5$ μm ($\gamma = 1.1 \times 10^{-2}$ kg m^{-1} s^{-1} at 19 °C). By (1), for this first passage time (t_k) and the relaxation time (τ), an average microtubule tip will bend at least $U_0 \approx 11\ kT$ (where $1\ kT = 4.0 \times 10^{-21}$ J at 19 °C). This corresponds to an approach angle of $\theta \approx 4°$. For guiding to occur, the microtubule approach angle must be at a shallow enough angle that this bending is enough to reach the adhesive glass region (Figure 7C). Because this represents only an average microtubule, we expect at this approach angle a guiding probability of 50%. In fact, we observe microtubule guiding at much larger angles with a guiding probability of $p = {}^1/_2$ at $\theta \approx 13°$.

Interestingly, eq 5 predicts nearly perfect guiding at small approach angles to the chemical edge, consistent with our observations. For microtubules aligned to the chemical edge, the fluctuating tip nearly always samples enough area to find the kinesin on the glass side of the edge. This is equivalent to the free tip needing only very slight bending on the order of a few kT, which will happen quite quickly as the first passage time for these small energies is small. Consequentially, chemical tracks are best arranged in straight narrow tracks (<1 μm in width) that bind only aligned microtubules and restrict the microtubule to shallow approach angles.

While our measurements have not included microtubules that are stuck and swiveling around nonmotile kinesin, a certain amount of swiveling may be occurring as the microtubule glides along the surface bound by few functional kinesin molecules. If a microtubule is driven by two motors spaced 300 nm away from one another along the microtubule and 20 nm of "play" (a fraction of the 70 nm overall length of kinesin),[35] they could allow the microtubule to change its angle 8° without detaching from the surface. A microtubule angle change of 8° over what is predicted by the bending theory (~4°) brings the expected approach angle where guiding will occur closer to the measured angle of $\theta \approx 13°$.

Our experiments use a high motor density to prevent detachment of microtubules from the surface. Although

(34) Mickey, B.; Howard, J. *J. Cell Biol.* **1995**, *130*, 909−917.
(35) Gibbons, F.; Chauwin, J. F.; Desposito, M.; Jose, J. V. *Biophys. J.* **2001**, *80*, 2515−2526.

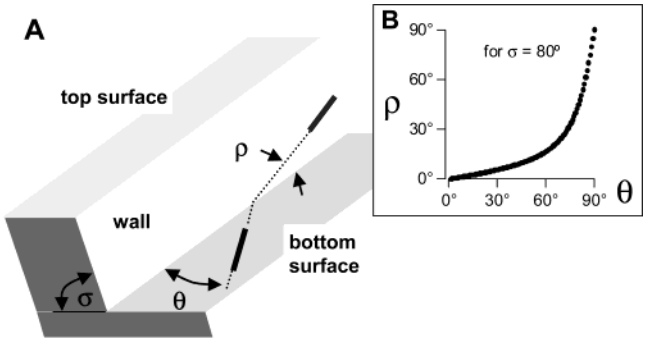

Figure 8. (A) The path of least bending is shown for a microtubule approaching a wall at an angle θ. For walls of steepness $\sigma < 90°$, the climbing angle ρ of the microtubule on the wall is less than the approach angle θ according to eq 6. (B) This relationship is plotted for topography-only polyurethane walls ($\sigma = 80°$).

lower motor densities with only one to two kinesin molecules bound per microtubule could exploit a swiveling mechanism[25,35] for guiding, the assays suffer from stochastic detachment of microtubules not related to boundary collisions. Therefore, guiding mechanisms at low motor densities are not presented in this paper.

Path of Least Bending for a Microtubule Traveling up a Wall. One way to understand how a wall may lead to guiding is to know how a wall changes the path of the microtubule. Walls cause microtubules to change their path either by bending them along the wall or by bending them up the wall, where they may or may not detach from the surface. Bending a microtubule requires energy, and therefore we may assume that microtubules follow an energetically favorable path that requires the smallest angle of bending. For walls of steepness $\sigma < 90°$, the climbing angle ρ of the microtubule on the wall is less than the approach angle θ and can be calculated by

$$\tan \rho = \tan \theta \cos \sigma \qquad (6)$$

where ρ is the climbing angle along the wall face with respect to the bottom surface, θ is the approach angle of the microtubule to the wall, and σ is the wall steepness as illustrated in Figure 8A.

For topography-only polyurethane surfaces, kinesin coats both walls, thereby enabling climbing of microtubules at angle ρ. To estimate the smallest value of ρ that is still considered guided by our selection criteria (microtubule remains in focus for 10 μm), we consider a microtubule that climbs the 1 μm high wall over a 10 μm distance. For a wall with steepness $\sigma = 80°$ (Figure 3), the wall face will have a width of $w = (1\ \mu\text{m}/\sin 80°) \approx 1\ \mu$m. Assuming a straight path for the microtubule, the climbing angle on the wall is approximately $\rho = \arctan(1\ \mu\text{m}/10\ \mu\text{m}) \approx 6°$. For smaller climbing angles, it becomes increasingly likely that the microtubule will lose its original direction of movement due to random fluctuations in its path, which results in a ~50% probability of returning to the bottom edge of the wall. For a wall with steepness $\sigma = 80°$, a value of $\rho = 6°$ corresponds to an approach angle of $\theta \approx 30°$ according to eq 6 (plotted as Figure 8B). This model corresponds well with experimental data where we observe approximately the same amount of guiding for $\theta < 30°$.

Larger approach angles lead to large climbing angles which are not generally guided as the microtubules climb the wall quickly and go out of focus or detach. Microtubule bending will vary statistically; there is a distribution of climbing angles for a single approach angle. However, this model correctly predicts that as the approach angle to a polyurethane wall increases, the probability of guiding decreases from a maximum of ~50% at shallow approach angles. At near orthogonal angles, the probability approaches zero as microtubules climb up the wall instead.

Combining topography and chemistry to make tracks for guiding, such as for SU8−PEO surfaces, may improve guiding due to the fact that kinesin is not adsorbed to the wall face and therefore cannot support microtubule climbing. A microtubule that bends to climb the wall and is still partially bound to the bottom surface will have its leading end free to sample the surface similar to the chemical boundary since it is unbound by kinesin. The nearest kinesin molecules are on the bottom surface and are an angle ρ away, due to the wall-induced bending of the microtubule according to eq 6 (shown in Figure 8A). The probability of the fluctuating end on the wall being guided can be estimated in the same way as for the chemical patterns, using the climbing angle ρ instead of the approach angle θ.

In fact, the steepness for combined patterns corresponds to $\sigma = 90°$ (Figure 3B) where we expect guiding at all angles as $\rho \rightarrow 0°$ and where guiding will always occur (according to eq 6). Our model agrees with qualitative observations of others[11] who note that steep walls and chemical selectivity were needed for frequent guiding of microtubules. The model predicts an increasing probability of guiding as the wall steepness increases.

The occasional microtubule that is not guided could be due to variation in the wall steepness. According to the model, we expect the climbing angle and therefore the guiding probability to fall for even a modest 5° decrease in wall steepness. Therefore, microtubule guiding may be sensitive to changes in wall steepness beyond our ability to measure it with the scanning electron microscope.

Prediction of Travel Distance for Straight Tracks. Previously we derived a relationship between guiding in collisions and microtubule travel distance in straight tracks of polyurethane.[19] Using this relationship, we can predict microtubule travel distances for chemical versus topography versus combined-patterning methods. The total distance traveled (d_{total}) along the track before escape in a nonguided collision is a sum of the initial distance to first collision (d_1) and distances between collisions (d_2)

$$\langle d_{\text{total}} \rangle = d_1 + d_2\left(\frac{p_{\text{guiding}}}{1 - p_{\text{guiding}}}\right) \qquad (7)$$

where p_{guiding} is the average probability of guiding for a collision with the track boundary. In our previous work[19] on 1.5 μm wide topography-only polyurethane channels, for example, we have measured d_1 and d_2 and the average approach angle as $11 \pm 8\ \mu$m, $16.6 \pm 7\ \mu$m, and $11° \pm 7°$, respectively. Assuming that these values are the same for all track types, the guiding probability corresponding to an approach angle of 11° in Figure 6 is estimated as $p_{\text{guiding}} \approx 0.59$, 0.56, and 0.87 for chemical-only, topography-only, and combined tracks, respectively. From eq 7, we predict $\langle d_{\text{total}} \rangle \approx 35$, 32, and 122 μm for chemical-only, topography-only, and combined straight tracks, respectively. Based on guiding probabilities at track boundaries, we plan to extend our model so that guiding in complex track shapes (i.e., curved tracks) can be predicted.

This analysis provides knowledge of when and where each patterning type may be useful as a molecular shuttle track through an understanding of the limitations of each

type. Chemical patterns are useful tracks when the microtubule/boundary crossings are limited to small approach angles,[19] where the guiding probability is nearly one ($p \approx 1$). Thus, for thin straight segments which limit the possible approach angles, chemical tracks will effectively transport filaments. For tight turns, microtubules will be approaching the boundary at larger angles; therefore combining walls with kinesin selectively adsorbed to the bottom surface may be the best option. Topography-only tracks may be useful when additional surface area is needed to capture a large number of microtubules in solution as in a sensing application.

Conclusion

This study determines quantitatively how chemical and topographical patterns on a surface can influence filament paths. We have also derived physical models that yield additional insight into the design of efficient tracks for motor protein shuttles. Our work may also shed light on cellular transport mechanisms where cargos must overcome obstacles in crowded cellular environments. By incorporating efficient tracks for molecular shuttles, we will be able to engineer simple nanoscale devices using complex track shapes.

Acknowledgment. The authors gratefully thank Emilie W. Clemmens for manuscript editing and comments. The authors acknowledge Jonathon Howard for the gift of GFP−kinesin, Nanotech User Facility for help with electron microscope images, and thank Buddy Ratner for use of the plasma deposition equipment. J.C. was supported in part by a fellowship from the Center of Nanotechnology (UIF) and an IGERT fellowship from the National Science Foundation (NSF). H.H. was supported in part by the Alexander-von-Humboldt Foundation. Y.H. was supported in part by NSF CISE EIA-0072744, and K.B. by NSF career award ECS-9875367. This work was funded by NASA Grant NAG5-8784, NIH Center of Excellence in Genomic Sciences 5-P50-HL-02360-02, and Packard Foundation Grant 2000-01763 and also partially supported through the Materials Science and Engineering Division, Office of Basic Energy Sciences, U.S. Department of Energy. Sandia is a multiprogram laboratory operated by Sandia Corporation, a Lockheed Martin Company, for the United States Department of Energy under Contract DE-AC04-94AL85000.

LA035519Y